

Impact of Climate Variability on the Ecological Components of a Swamp: the Case of Pantanos De Villa, Peru

Dagnert L. Naquiche Yesquen^a, Kenia K. Luna Ayala^a, Carlos A. Castañeda Olivera^{a,*}, Jorge L. Jave Nakayo^{a,b}, Jhonny W. Valverde Flores^a, Eduardo R. Espinoza Farfán^a

^a Universidad César Vallejo, Campus Los Olivos, Lima, Peru

^b Universidad Nacional Mayor de San Marcos, Lima, Perú
caralcaseo@gmail.com

The different ecological components of fragile ecosystems in the Pantanos de Villa Wildlife Refuge are naturally affected by fluctuations in climate variability, mainly due to climatological elements. The impact of vegetation by climatic variability was determined based on the normalized difference vegetation index (NDVI) with climatic data for the dry season from 2000 to 2020 (May). The results showed an increasing trend in the NDVI during the study period. Vegetation was most vigorous in 2020 with an NDVI of 0.548. Likewise, in the summer season, vegetation cover had an inverse association with correlation values of -0.323, -0.252, -0.138 and -0.270 for temperature, precipitation, humidity and insolation, respectively. In addition, using Landsat 7 ETM+, Landsat 8 OLI satellite imagery and geographic information systems (GIS), 8 vegetation units were identified in the wetland, which were dominated by a greater distribution of desert saltgrass (*Distichlis spicata*). From the results, it was concluded that some climatic elements have a greater impact on the ecological components, especially on vegetation.

1. Introduction

Climate variability puts wetland biodiversity at risk, evidencing significant changes in the geographic relief, vegetation covers and water bodies, unbalancing the ecological functions, geochemical cycles, carbon sequestration and environmental services provided by wetlands (Shand et al., 2017). This variability is linked to climate change because it influences the interaction of species with their natural environment, generating an imbalance in reproduction, migration and taxonomy (Miller et al., 2018). This phenomenon manifests itself naturally through fluctuations in climatic variables at the regional or local level. It also causes extreme events such as droughts, floods, cold and heat waves, and heavy rainfall (Butterfield et al., 2020). Remote sensing has been shown to be a tool to monitor and map the spatio-temporal dynamics of fragile ecosystems, mainly vegetation cover caused by climatic variables (Zhu et al., 2020). NDVI as part of remote sensing is used to estimate changes in wetlands and to provide information, monitoring and assessment of the growth status of vegetation cover affected by climatic variables such as temperature, precipitation and evapotranspiration that influence arid, semi-arid and wetland regions (Piedallu et al., 2019). Remote sensing, by processing satellite images such as Landsat ETM, OLI, MSS (Yang et al. 2020), MODIS (Li and Xiao, 2020), CBERS-2B - CBERS-4 (Flores, 2019) and Sentinel 2A (Li et al. 2019) allows the mapping of changes in different types of wetlands (Wang et al., 2020). In addition, these images are able to differentiate vegetation covers and units such as plantations, grasslands, shrubs, wetlands, agricultural areas, and bamboo forests (Singh et al., 2020). Wetlands (carbon sinks) are considered climate regulators, vulnerable to the effects induced by climatic variables (Mohamed et al., 2020). This fragile ecosystem is formed by abiotic and biotic components that interact with each other and is one of the most productive ecosystems on the planet (Hernández and Muñoz, 2018). Therefore, this research focused mainly on determining the impact of climate variability on the ecological components of the Pantanos de Villa in Peru, mainly on the vegetation cover, considering climatic elements such as precipitation, humidity, temperature and insolation in the NDVI. In addition, to determine the

effect of climate variability on the identification of vegetation units present in the study area during the summer season from 2000 to May 2020.

2. Materials and methods

2.1 Study area

The Pantanos de Villa Wildlife Refuge is a wetland located in the Chorrillos district of Peru. It is geographically located 12°10'- 12°13' S; 77° 01'-77°02' W, between 0 and 15 m.a.s.l., with an approximate extension of 263.27 ha (Pulido, 2018). The climatic condition is arid because it is located in the coastal strip; during the summer season there is a monthly rainfall with values of 0 to 5.5 mm, the temperature ranges from 15.6 to 26 °C, in the month of February there is an average relative humidity of 86%, in the winter season the temperature ranges from 14 to 19 °C and in August there is a maximum relative humidity of 92% (Garrote et al., 2020).

2.2 Data sets

The data of the climatic variables (precipitation, temperature, humidity and insolation) were obtained from the National Service of Meteorology and Hydrology of Peru (SENAMHI) and the National Water Authority (ANA) of the Peruvian state. In addition, data from NASA's POWER project was used to complete the database of the variables studied. A total of 21 scenes were collected from two sets of Landsat images (ETM and OLI) acquired from the United States Geological Survey (USGS) platform.

2.3 Landsat image processing

Pre-processing was done, which consists of correcting or calibrating the images to minimize errors. The corrections were made using ENVI 5.1 software. The radiometric correction allowed to improve the imperfections of each pixel, and the atmospheric correction allowed to eliminate the cloud cover (cirrus clouds). This last correction was made through the FLAASH (Fast Line-of-sight Atmospheric Analysis of Spectral Hypercubes) module. Subsequently, the corrected images were processed with ArcGIS 10.8 software through supervised classification. Ten representative points or training sites were chosen along the raster image to group the pixels with the same spectral signature, differentiating the different types of vegetation units. To validate the whole process, the maximum probability method was applied.

2.4 Calculation of NDVI and identification of vegetation units

NDVI is related to vegetation conditions in the wetland. It is a numerical indicator whose range of variation is -1 and +1, where positive values correspond to vegetation zones and negative values correspond to soil and water. To calculate the NDVI, the multispectral band combination method was applied according to each Landsat version. To facilitate the analysis of NDVI values, ranges from -1 to 0 were chosen for the non-vegetation class, from 0 to +0.25 for the mixed vegetation class and from +0.25 to +1 for the dense vegetation class. To map the NDVI dynamics present in the study area, the raster format was converted to a shapefile (shp). NDVI calculations for Landsat ETM and Landsat OLI satellites were performed using equation (1) and equation (2), respectively (Roy et al., 2016).

$$NDVI = \frac{Psb4 - Psb3}{Psb4 + Psb3} \quad (1)$$

$$NDVI = \frac{Psb5 - Ps b4}{Psb5 + Ps b4} \quad (2)$$

Where, Ps b4 and Ps b3 correspond to the near infrared and red band of the Landsat 7 ETM version, respectively. Ps b5 (near infrared) and Ps b4 (red band) belong to Landsat 8 OLI.

On the other hand, the vegetation units were identified by means of the supervised classification that was executed using ArcGIS 10.8 software. This classification uses spectral signatures of the raster bands of the processed images in order to extract information from each vegetation unit found.

3. Results and discussion

3.1 Impact of climate variables on the NDVI

The results revealed that the climatic variables generated a slight increase in vegetation within the wetland (Table 1). In the year 2000, areas with little vegetation and presence of water bodies were shown, obtaining an NDVI value of -0.057. For the years 2005, 2010, 2015 and 2020, NDVI values increased to 0.153, 0.359, 0.431 and 0.767, respectively, indicating greater vegetation in the areas. However, this does not mean that

vegetation is in suitable condition, because climate variability can influence vegetation growth and development (Ley et al., 2018). It has been documented that in dry seasons, variations in climatic variables have an effect on changes and expansion of vegetation cover by increasing NDVI values (Yang et al., 2020). Rainfall during the summer season does not exceed 7 mm, showing anomalies and a downward trend from 2000 to 2014. In 2015, rainfall increased to a maximum of 6.08 mm, while in 2020, a significant decrease was observed (0.35 mm). Even under low rainfall conditions, NDVI continued to increase slightly to approach the value of 1 (dense vegetation), with a correlation of -0.323, indicating a low negative relationship.

Temperature had a negative correlation of -0.252, the behavior of this climatic variable slightly increased NDVI values, and consequently influenced the slight increase in vegetation during the summer. For the years 2000, 2005, 2010, 2015 and 2020, the temperature values were 20.7, 21, 19.3, 18.9 and 22.2°C, respectively, registering its highest value in the last year of study. These results are in contradiction with Chu (2019), who showed that NDVI in the summer season had positive correlations with temperature.

Humidity in the summer season showed a gradual decrease from 2000 onwards. However, from 2015 to 2020 it increased significantly from 70.7 to 77.5%, respectively, allowing water absorption in vegetation, and as a consequence, NDVI presented a very low negative association with a value of -0.138. According to Piedallu et al. (2019), humidity causes greenness in vegetation reflected in NDVI values. Other factors such as evapotranspiration and precipitation allow vegetation cover to modify the extent of other ecosystems and even biodiversity (Zhu et al., 2019).

In 2000, 2005, 2010 and 2015, insolation presented similar values which were 19.81, 19.91, 19.12 and 19.39 MJ/m², respectively. Already in 2020 there was a decrease (18.21 MJ/m²), showing a low negative correlation of -0.270.

On the other hand, the changes experienced by wetlands are reflected in the degradation of ecological components that are caused by anomalies in climatic variables (Shen et al, 2019).

Table 1: Values of climate variables, NDVI and Spearman correlation

Summer season		Climatic variables			
year	NDVI value	Precipitation (mm)	Temperature (°C)	Humidity (%)	Sunshine (MJ/m ²)
2000	-0.057	2.62	20.7	72.8	19.81
2005	0.153	1.17	21.0	70.8	19.91
2010	0.359	1.14	19.3	70.2	19.12
2015	0.431	6.08	18.9	70.7	19.39
2020	0.767	0.35	22.2	77.5	18.21
Spearman correlation		-0.323	-0.252	-0.138	-0.270

3.2 NDVI distribution and spatial dynamics

The vegetation evolution of the wetland was mapped for the years 2000, 2005, 2010, 2015 and 2020. Figure 1 shows the maps of the three vegetation classes obtained by NDVI and the variations that occurred during the study period. The results revealed that dense vegetation had a positive evolution occupying larger areas within the wetland, i.e., a higher concentration of plant biomass. Likewise, the mixed vegetation class had a positive trend in the surface of the study area. Meanwhile, the non-vegetation class showed a decreasing trend allowing the decrease of areas with scarce vegetation and different areas occupied by other components (bare soil and water bodies), as shown in Table 2.

Table 2: Values of the three vegetation classes for the period 2000 to 2020

Summer season	2000		2005		2010		2015		2020	
Vegetation classes	Area (km ²)	%	Area (km ²)	%	Area (km ²)	%	Area (km ²)	%	Area (km ²)	%
Non-vegetation	2.284	86.85	1.469	55.86	0.792	30.11	0.668	25.39	0	0
Mixed vegetation	0.334	12.90	1.163	44.14	1.272	48.34	1.633	62.10	1.440	54.77
Dense vegetation	0.004	0.24	0	0	0.558	21.53	0.319	12.48	1.178	45.23

Figure 4 shows the variation of the three vegetation classes. In 2000 (see Figure 4-a), the area of the non-vegetation class (represented in yellow) is 2.284 km² (86.85%) and presents an NDVI value of -0.264 that

shows the presence of water bodies, arid soils and areas of low vegetation cover. Mixed vegetation is the second most present class within the wetland, with an area of 0.334 km² (12.90%). Meanwhile, the dense vegetation class had too small an area of 0.004 km² (0.24%).

The dense vegetation class was not present in 2005 (Fig. 4-b), registering a null value, while mixed vegetation increased its area to 1.163 km² (44.14%), and the extent of the non-vegetation class decreased to 0.792 km² (30.11%).

Figure 4-c shows that in 2010 there was an increase in the areas of the dense and mixed vegetation classes, with values of 0.558 and 1.272 km², respectively. Meanwhile, the area of the non-vegetation class decreased to 0.792 km².

In 2015 (Fig. 4-d), the wetland had an increase in the area of mixed vegetation (1.633 km²), a slight decrease in the area of dense vegetation (0.319 km²) and a lower predominance of the non-vegetation class (0.792 km²).

By 2020 (Fig. 4-e), Pantanos de Villa was mostly occupied by the mixed (1,440 km²) and dense (1,178 km²) vegetation classes, with NDVI values of 0.219 and 0.548, respectively.

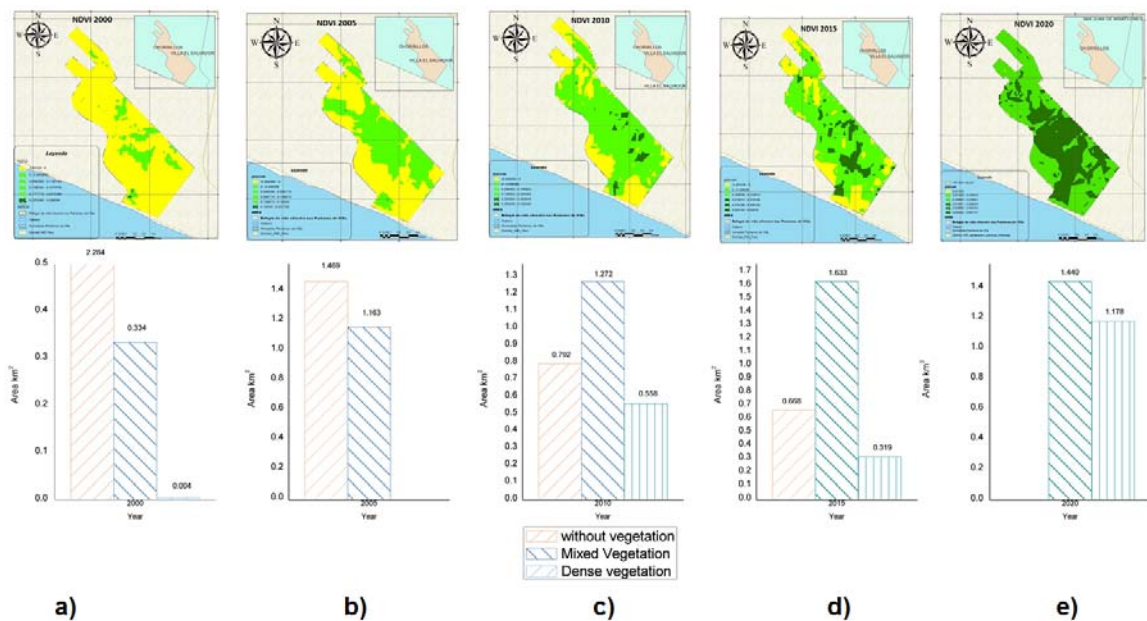


Figure 1: Variation of the three vegetation classes: a) NDVI 2000, b) NDVI 2005, c) NDVI 2010, d) NDVI 2015 and e) NDVI 2020

A study conducted in a geographically similar context found that mixed vegetation occupied the greatest extent of the wetland during the years 2004 to 2018, however the areas of sparse vegetation were increasing due to the reduction of dense vegetation caused by different land uses and anthropogenic activities (Flores, 2019).

3.3 Identification of vegetation units

Table 3 shows the eight vegetation units identified by the two Landsat versions. The Landsat 7 (ETM+) image set identified 3 vegetation units including cumbungi (*Typha domingensis*), desert saltgrass (*Distichlis spicata*) and Chairmaker's bulrush (*Schoenoplectus americanus*). *Typha domingensis* is a species found in many wetlands and its ecological function is to improve the quality of water bodies as well as to restore fragile ecosystems (Eid et al. 2020). *Distichlis spicata* was most prevalent in the Pantanos de Villa, and is a species that grows in environments with saline soils (León et al., 1995). *Schoenoplectus americanus*, this species is found among aquatic grasses and saline soils with saltgrass (SERNANP, 2016).

On the other hand, with Landsat 8 (OLI) five vegetation units were digitally identified throughout the wetland, including: the species Salicornias (*Salicornia fruticosa*), a halophyte tolerant to high soil salinity levels and that can survive in arid areas (Marco et al., 2019); reed (*Phragmites australis*), a neophyte that grows in very wet soils (Jaklič et al, 2020); water lettuce (*Pistia stratiotes*), a floating aquatic macrophyte found in water channels (Jaklič, Koren and Jogan 2020); floating pennywort (*Hidrocotyle ranunculoides*), another aquatic species

found in slow-flowing waters (León and Sáenz 2020) and sawgrass (*Cladium Jamaicense*) which is a macrophyte that contributes to wetland restoration (Pulido et al. , 2020).

Previous studies have mapped wetlands as deciduous, coastal and other evergreen wetlands (Wang et al, 2020). In addition, other studies indicate that smaller-scale satellite image processing allows for differentiation of vegetation cover such as plantation, grasses, shrubs, wetlands, and agricultural areas (Singh et al., 2020), including bamboo forests (Li et al. 2019).

Table 3: Vegetative units identified with Landsat ETM and OLI

Summer season		
Satellite / sensor	Vegetative unit	Scientific name
Landsat ETM / Landsat OLI	Desert saltgrass	<i>Distichlis spicata</i>
	Chairmaker's bulrush	<i>Schoenoplectus americanus</i>
	Reed	<i>Phragmites australis</i>
	saw-grass	<i>Cladium Jamaicense</i>
	Cumbungi	<i>Typha domingensis</i>
	Salicornias	<i>Salicornia fruticosa</i>
	floating pennywort	<i>Hydrocotyle Ranunculoides</i>
	Water lettuce	<i>Pistia stratiotes</i>

4. Conclusions

The research determined through mapping the impact of climate variability on the ecological components of the Pantanos de Villa. It was demonstrated that climate variability generates positive and negative impacts on vegetation, which was evidenced in the normalized difference vegetation index (NDVI). In addition, it was shown that the mixed vegetation had a greater area with respect to dense vegetation and non-vegetation. A total of eight vegetative units were also identified, with the species *Distichlis spicata* having the greatest presence in the Pantanos de Villa.

Acknowledgments

The authors would like to thank Universidad César Vallejo for the academic and technical support in carrying out the research.

References

- Butterfield Z., Buermann W., Keppel-Aleks G., 2020, Satellite observations reveal seasonal redistribution of northern ecosystem productivity in response to interannual climate variability, *Remote Sens. Environ*, 242, 111755.
- Chu H., Venevsky S., Wu C., Wang M., 2019, NDVI-based vegetation dynamics and its response to climate changes at Amur-Heilongjiang River Basin from 1982 to 2015, *Sci, Total Environ*, 650, 2051–2062.
- Duarte Hernández D., Avella Muñoz E.A., 2018, Análisis socio-ecológico de una iniciativa de restauración liderada por autoridades ambientales en Santander, Colombia, *Colomb, For*, 22, 68–86.
- Eid E.M., Galal T.M., Shaltout K.H., El-Sheikh M.A., Asaeda T., Alatar A.A., Alfarhan A.H., Alharthi A., Alshehri A.M.A., Picó Y., Barcelo D., 2020, Biomonitoring potential of the native aquatic plant *Typha domingensis* by predicting trace metals accumulation in the Egyptian Lake Burullus, *Sci, Total Environ*, 714, 136603.
- Flores, Nathalie E. F., 2019, Evaluación de las unidades de vegetación mediante sistemas de información geográfica y teledetección en Pantanos de Villa, Chorrillos - Lima. Univ. Católica Sedes Sapientiae 27.
- Garrote J., Ruiz V., Troncoso O.P., Torres F.G., Arnedo M., Elices M., Pérez-rigueiro J., 2020, Application of the Spider Silk Standardization Initiative (S3I) methodology to the characterization of major ampullate gland silk fibers spun by spiders from Pantanos de Villa wetlands (Lima, Peru), *J Mech Behav Biomed Mater*, 104023.
- Jaklič M., Koren Š., Jogan N., 2020, Alien water lettuce (*Pistia stratiotes* L.) outcompeted native macrophytes and altered the ecological conditions of a Sava oxbow lake (SE Slovenia), *Acta Bot Croat*, 79, 35–42.
- León B., Cano A., Young K., 1995, La Flora Vasculare de los Pantanos de Villa, Lima, Perú: Adiciones y guía para las especies comunes, *Mus. Hist. Nat. UNMSM*, 1–39.

- León J.C., Sáenz, P.S., 2020, Floristic inventory and vegetation of the crater of the Alberca de Teremendo, Michoacan, Mexico, *Acta Bot Mex*, 2020, 1–23.
- Ley A.C., Herzog P., Lachmuth S., Abwe A.E., Christian M.F., Sesink Clee P.R., Abwe E.E., Morgan B.J., Gonder M.K., 2018, Phenotypic variability along a climatic gradient in a perennial afro-tropical rainforest understorey herb, *Basic Appl. Ecol*, 28, 60–75.
- Li L., Li N., Lu D., Chen Y., 2019, Mapping Moso bamboo forest and its on-year and off-year distribution in a subtropical region using time-series Sentinel-2 and Landsat 8 data. *Remote Sens Environ*, 231, 111265.
- Li X., Xiao J., 2020, Global climatic controls on interannual variability of ecosystem productivity: Similarities and differences inferred from solar-induced chlorophyll fluorescence and enhanced vegetation index, *Agric For Meteorol*, 108018.
- Marco P., Carvajal M., Martínez-Ballesta M. del C., 2019. Efficient leaf solute partitioning in *Salicornia fruticosa* allows growth under salinity, *Environ Exp. Bot*, 157, 177–186.
- Miller D.A.W., Grant E.H.C., Muths E., 2018, Quantifying climate sensitivity and climate-driven change in North American amphibian communities, *Nat. Commun*, 9, 1–15.
- Nasser Mohamed Eid A., Olatubara C.O., Ewemoje T.A., Farouk H., El-Hennawy M.T., 2020, Coastal wetland vegetation features and digital Change Detection Mapping based on remotely sensed imagery: El-Burullus Lake, Egypt, *Int. Soil Water Conserv. Res*, 8, 66–79.
- Piedallu C., Chéret V., Denux J.P., Perez V., Azcona J.S., Seynave I., Gégout J.C., 2019, Soil and climate differently impact NDVI patterns according to the season and the stand type, *Sci. Total Environ*, 651, 2874–2885.
- Pulido C., Sebesta N., Richards J.H., 2020, Effects of salinity on sawgrass (*Cladium jamaicense* Crantz) seed germination, *Aquat. Bot*, 103277.
- Pulido V., 2018, One hundred and fifty years of keeprecords from Pantanos de Villa birds' [Ciento quince años de registros de aves en Pantanos de Villa], *Rev. Peru. Biol*, 25, 291–306.
- Roy, D.P., Kovalsky, V., Zhang, H.K., Vermote, E.F., Yan, L., Kumar, S.S., Egorov, A., 2016. Characterization of Landsat-7 to Landsat-8 reflective wavelength and normalized difference vegetation index continuity, *Remote Sens. Environ*, 185, 57–70.
- Servicio Nacional de Áreas Naturales Protegidas por el Estado (SERNANP), 2016, Plan Maestro: Pantanos de Villa Refugio de Vida Silvestre. 2016. S.I.: s.n.
- Shand P., Grocke S., Creeper N.L., Baker A.K., Fitzpatrick R.W., Love A.J., 2017, Impacts of Climate Change, Climate Variability and Management on Soil and Water Quality in Wetlands of South Australia, *Procedia Earth Planet, Sci*, 17, 456–459.
- Shen G., Yang X., Jin Y., Xu B., Zhou Q., 2019, Remote sensing and evaluation of the wetland ecological degradation process of the Zoige Plateau Wetland in China, *Ecol. Indic*, 104, 48–58.
- Singh S., Bhardwaj A., Verma V.K., 2020, Remote sensing and GIS based analysis of temporal land use/land cover and water quality changes in Harike wetland ecosystem, Punjab, India, *J. Environ. Manage*, 262, 110355.
- Wang X., Xiao X., Zou Z., Hou L., Qin Y., Dong J., Doughty R.B., Chen B., Zhang X., Chen Y., Ma J., Zhao B., Li B., 2020, Mapping coastal wetlands of China using time series Landsat images in 2018 and Google Earth Engine, *ISPRS J. Photogramm. Remote Sens*, 163, 312–326.
- Yang L., Wang, Lunche Yu, D., Yao R., Li C., He Q., Wang S., Wang, Lizhe, 2020, Four decades of wetland changes in Dongting Lake using Landsat observations during 1978-2018, *Journal of Hydrology, Elsevier B.V.*
- Zhu Y., Zhang J., Zhang Y., Qin S., Shao Y., Gao, Y., 2019, Responses of vegetation to climatic variations in the desert region of northern China, *Catena* 175, 27–36.